



Research Article

Anomaly Detection of Pipeline Leakage Based on Electric Field Component Imaging Using Ground Penetrating Radar

Yang Yang ¹, Zhiyuan Du,² Yanan Li,¹ Tianyu Zhang,¹ Lu Liu,¹ Ibrar Iqbal,¹
and Sanxi Peng ¹

¹College of Earth Sciences, Guilin University of Technology, Guilin, Guangxi, China

²Taiyuan Mingshida Coal Design Co. Ltd., Taiyuan, Shanxi, China

Correspondence should be addressed to Sanxi Peng; pengsanxi1984@163.com

Received 28 March 2022; Accepted 16 June 2022; Published 27 June 2022

Academic Editor: Ma Jianjun

Copyright © 2022 Yang Yang et al. This is an open access article distributed under the Creative Commons Attribution License, which permits unrestricted use, distribution, and reproduction in any medium, provided the original work is properly cited.

Ground penetrating radar (GPR) is an effective method that can be applied in pipeline leakage detection. However, when the distribution of the underground medium is complex, it becomes difficult to accurately identify the abnormal leakage area directly from the GPR data profile. In this paper, based on the characteristics of high water content in the abnormal leakage area and according to the relationship between the reflected wave coefficient and the dielectric constant, the electric field component imaging technology of GPR data is proposed. Next, the electromagnetic wave responses of geological models with different dielectric parameters are simulated by finite difference time domain (FDTD). It can be seen from the forward modeling results that the greater the difference is in the dielectric constants of the media on both sides of the interface, the stronger the reflected wave energy will be. Finally, the electric field component imaging technology of GPR data is applied to pipeline leakage detection in an industrial area. The test results show that the abnormal area of pipeline leakage appears as a high-amplitude area in the electric field component map.

1. Introduction

Leakage detection of underground pipelines is an important task of municipal engineering. Ground penetrating radar (GPR) is a geophysical method that applies the propagation characteristics of high-frequency electromagnetic waves (such as reflected, transmitted, and refracted waves) to detect underground media. The detection results have high resolution and strong intuition and are widely applied in shallow surface detection projects [1, 2].

In recent years, GPR has achieved promising results in underground pipeline detection [3–5]. However, there remain some difficulties in pipeline leakage detection due to the fact that the complex underground structure of the pipeline leakage area makes it difficult to identify abnormal GPR data. The anomaly identification of GPR data is the key to the interpretation process [6], while reasonable imaging technology is the basis of anomaly identification. In leakage detection engineering, GPR processing software is typically

used to edit, correct, gain, and filter the original data, after which the abnormal leakage area can be determined according to the energy intensity of the GPR profiles. Throughout the entire GPR data processing flow, the value of the electric field component signal is unknown, and sometimes, false strong signals are introduced in the data processing process. These disturbances may lead to incorrect GPR interpretation results. For example, when the GPR data quality is not ideal or the leakage area is small, then horizontal noise signals introduced by gain and filtering can interfere with anomaly identification. The water content in the leakage area of the pipeline is high, and there is a large difference in the relative permittivity between the seepage water and the surrounding soil. Considering these points, and based on the theoretical basis that the reflected wave energy of electromagnetic waves is related to the difference in the relative permittivity of the medium, this paper proposes the electric field component imaging technique for GPR data. The electric field component imaging technology

extracts the electric field intensity value of the radar data. After simple data processing, the abnormal reflection area can be visually identified according to the size of the detection value. Therefore, the electric field component imaging technology maintains the authenticity of the data and improves the accuracy of data interpretation.

In this paper, the relationship between electromagnetic wave reflection coefficient and relative permittivity is deduced, and the correctness of the theoretical basis is verified by means of finite difference time domain (FDTD). Finally, taking the pipeline leakage detection project in an industrial area as an example, the measured GPR data are analyzed by using the electric field component imaging technology and the abnormal area is delineated. The results are satisfactory, which verifies the effectiveness of the method.

2. Methodology

In GPR detection, the transmitting antenna radiates the electromagnetic field outward, the receiving antenna receives the scattered electromagnetic waves in the detection area and converts them into electrical signals, and finally, the computer completes the data storage, processing, and display. In pipeline leakage detection, the effective data of GPR are the reflected electromagnetic wave of the underground medium and the difference of dielectric constant will cause the change in the reflected wave energy. In this paper, the relationship between electromagnetic wave reflection coefficient and relative permittivity is deduced. This in turn provides a theoretical basis for the application of electric field component imaging technology to pipeline leakage detection.

According to the research results of Wu et al. [7], on the interface of the medium, the reflection coefficients of the transverse electric field component (TE wave) and the transverse magnetic field component (TM wave) of the electromagnetic wave can be, respectively, expressed as formulas as follows:

$$R_{TE} = \frac{(Z_2 / \cos \theta_2) - (Z_1 / \cos \theta_1)}{(Z_2 / \cos \theta_2) + (Z_1 / \cos \theta_1)}, \quad (1)$$

$$R_{TM} = \frac{Z_2 \cos \theta_2 - Z_1 \cos \theta_1}{Z_2 \cos \theta_2 + Z_1 \cos \theta_1}, \quad (2)$$

where R_{TE} and R_{TM} are the reflective coefficients of TE and TM waves, respectively, and Z_1 and Z_2 are the wave impedances of Medium 1 and Medium 2, which should satisfy the following formula:

$$\begin{aligned} Z_1 &= \sqrt{\frac{\mu_1}{\varepsilon_1 \varepsilon_0}}, \\ Z_2 &= \sqrt{\frac{\mu_2}{\varepsilon_2 \varepsilon_0}}. \end{aligned} \quad (3)$$

The underground medium can generally be considered to be nonmagnetic. Therefore, the magnetic permeability of the medium is equal to the magnetic permeability in vacuum, i.e., $\mu_1 = \mu_2 = \mu_0 = 1.25 \times 10^6 \text{ H/m}$, where ε_1 and ε_2 are

the relative permittivities of Medium 1 and Medium 2, respectively.

In most cases, the transmit-receive distance of GPR antenna can be considered to be very small relative to the depth of the reflection interface; thus, it is practical to study the normal incidence of electromagnetic waves. When the electromagnetic wave transmits vertically into the interface, then the reflection coefficients of the TE wave and the TM wave are the same. Then, formulas (1) and (2) can be simplified as follows:

$$R = \frac{Z_2 - Z_1}{Z_2 + Z_1}. \quad (4)$$

Substituting formula (3) into (4), we obtain the following:

$$R = \frac{1 - \sqrt{\varepsilon_2 / \varepsilon_1}}{1 + \sqrt{\varepsilon_2 / \varepsilon_1}} \quad (5)$$

Defining k as the coefficient of difference in permittivity of two media, i.e., $k = \sqrt{\varepsilon_2 / \varepsilon_1}$, we obtain the following:

$$R = \frac{1 - k}{1 + k}. \quad (6)$$

If the direction of the reflection coefficient is not considered and only its magnitude is considered, then we obtain the following:

$$|R| = \begin{cases} \frac{1 - k}{1 + k}, & 0 < k \leq 1, \\ \frac{k - 1}{1 + k}, & k > 1. \end{cases} \quad (7)$$

From formula (7), we determine the following:

- (1) When $0 < k < 1$, i.e., $\varepsilon_2 < \varepsilon_1$, then $|R|$ is a decreasing function, and the smaller $\varepsilon_2 / \varepsilon_1$ is, the larger $|R|$ will be
- (2) When $k > 1$, i.e., $\varepsilon_2 > \varepsilon_1$, then $|R|$ is an increasing function, and the larger the $\varepsilon_2 / \varepsilon_1$ is, the larger $|R|$ will be

In summary, the greater the difference between the relative permittivities ε_1 and ε_2 of the medium is, the greater the value of the reflection coefficient will be. In addition, the greater the difference in the relative permittivity is, the greater the reflected wave energy will be, namely, the greater the value of the electric field component will be.

In pipeline leakage detection, the leakage area has the characteristics of high water content. It can be seen from Table 1 that the dielectric constant of water is much higher than that of the medium in the other nonleakage areas (i.e., the difference in dielectric constant in the seepage area is large) and the reflected wave energy in the seepage area is stronger than that in other areas. Based on the above theoretical basis, the leakage area can be determined according to the magnitude of the electric field component of the reflected wave of the GPR data.

The essence of the electric field component is the electric field strength extracted from the electrical signal of the GPR data. Since the leakage water and the surrounding dielectric

TABLE 1: Dielectric constants of common media.

Type of medium	Dielectric constant
Air	1
Pure water	81
Asphalt (dry)	2–4
Asphalt (wet)	10–20
Plastic	3
Concrete	4–20
Soil	2–25

constant differ significantly, the electric field component of the reflected wave in the abnormal leakage area will also be much higher than those in other areas. Before extracting the electric field component, the authenticity of the data must be ensured and no gain or 2D filtering may be performed on it. In addition, the electric field component of the GPR data must be normalized to highlight high- and low-amplitude regions in the spectrum.

3. Forward Modeling Example

Forward modeling is an effective way to understand the theoretical derivation. In order to verify the relationship between the reflection coefficient and the relative permittivity difference, the FDTD method is used to simulate the energy characteristics of the GPR reflected waves corresponding to the models with different relative permittivities, thereby providing theoretical support for the electric field component imaging technology of GPR data. The FDTD algorithm is a commonly used GPR forward modeling method. This method is based on the Maxwell equation, replaces the differential equation containing the electric field component E and the magnetic field component H with a discrete difference equation, and obtains the electromagnetic field by means of alternate sampling [8–11].

As shown in Figure 1, in the forward modeling model, the dimensions of the model are 5×3 m and the background relative permittivity is set to 5. Anomaly body 1 has dimensions of 2×0.2 m, and its relative permittivity is 50, while Anomaly body 2 has dimensions of 2×0.2 m, and its relative permittivity is 20. The conductivity of the entire model is set to 0.001 S/m. Detecting parameters: the center frequency of the transmitting antenna is 400 MHz; the transmitting and receiving distance of the antenna is 0.2 m; the offset distance of the surveying point is 0.2 m; the horizontal distance of the surveying line is 0.1–4.5 m; and there are a total of 23 surveying points.

The forward modeling profile of the E_z component is shown in Figure 2, in which the electric field component value is a normalized value. The direct wave has been removed, so as to highlight the energy of the reflected wave. The following can be seen from Figure 2: (1) The reflected waves on the upper interface of Anomaly body 1 and Anomaly body 2 both occur at 20 ns, and the reflected wave energy E_1 of Anomaly body 1 is clearly stronger than that of Anomaly body 2. (2) The reflected wave from the lower interface of Anomaly body 1 occurs at 35 ns, and the lower interface of Anomaly body 2 occurs at 30 ns. E_1 is slightly

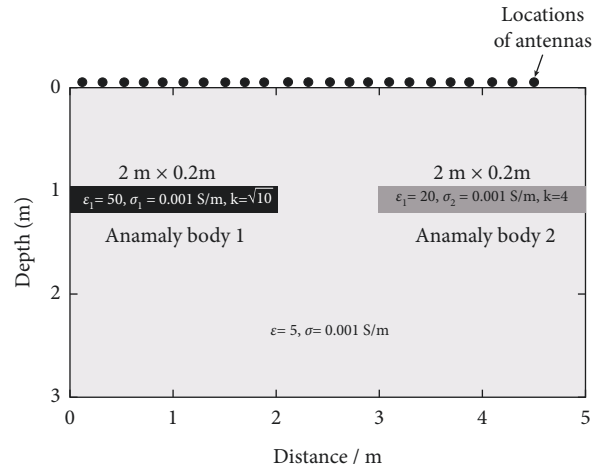


FIGURE 1: Diagram of the forward simulation model. The electromagnetic wave transmits vertically into the interface, and the transmitting and receiving antennas are in the same place at each surveying point.

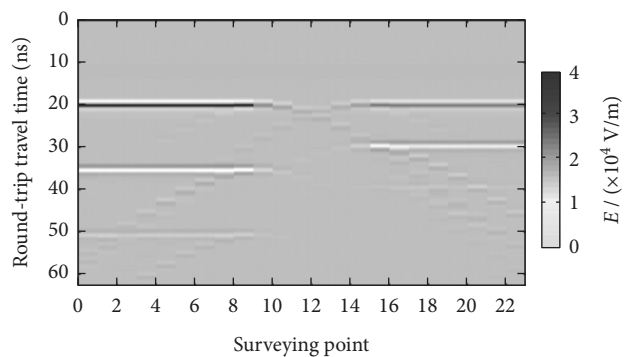


FIGURE 2: Forward simulation results of the electric field component (after removing direct waves), where (E) refers to “electric field component.”

stronger than E_2 , and the wave speed v_1 is lower than v_2 . (3) The multiple reflective wave of Anomaly body 1 occurs at 50 ns, the multiple transmitting wave of Anomaly body 2 occurs at 40 ns, and E_1 is significantly stronger than E_2 .

In summary, the forward modeling result proves that the greater the difference in dielectric constant is, the greater the reflection coefficient value will be and the greater the electric field component will be.

4. Experimental Study

There is abnormal pipeline leakage in an industrial area, which is selected to be the study area. MALA ground penetrating radar with a 250 MHz antenna is used to detect pipeline leakage in this area, and the continuous acquisition mode of a ranging wheel is used to collect data. One surveying line and one complementary line are arranged, and the complementary line is located 1 m to the left of the surveying line. The surveying line is 18 m in length and the complementary line is 5 m in length. Both lines are arranged perpendicular to the pipeline direction (Figure 3).

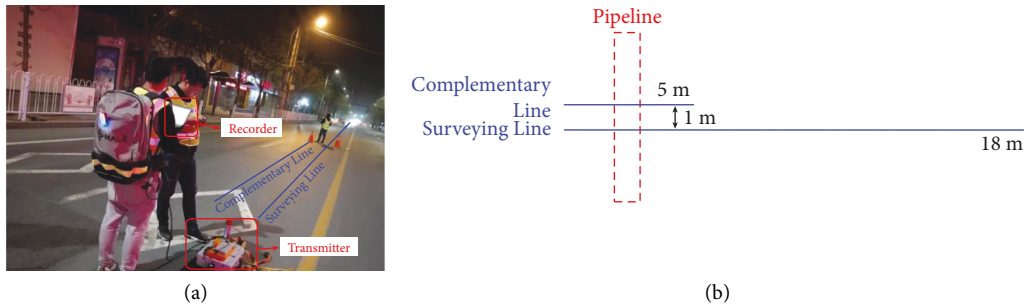


FIGURE 3: Data acquisition for pipeline leakage survey: (a) experimental setup for synthetic data; (b) schematic diagram for the detecting lines.

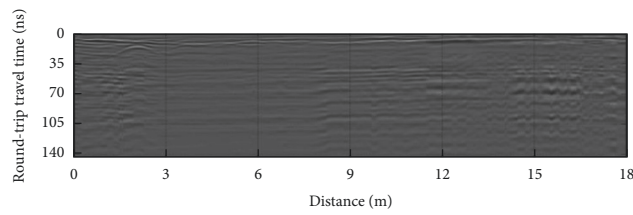
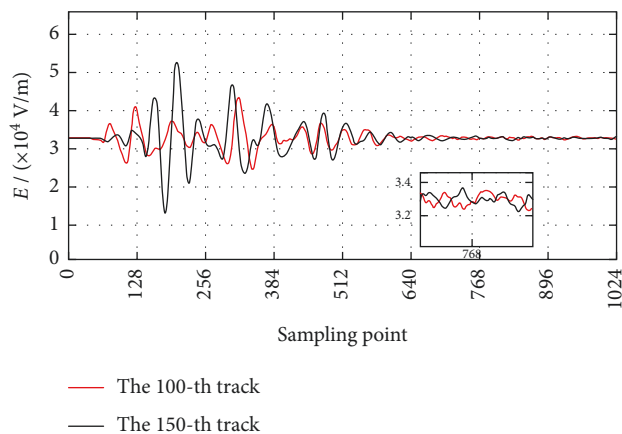
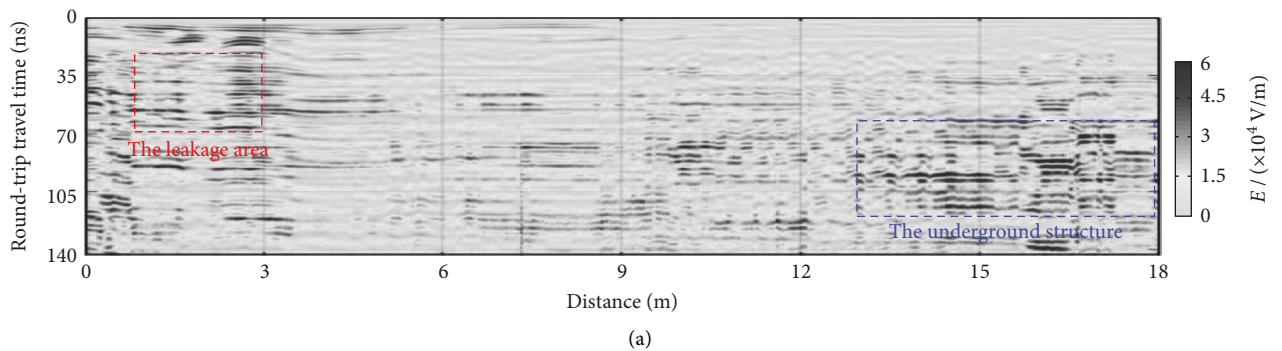


FIGURE 4: GPR profile of the surveying line.



(b)

(c)

FIGURE 5: Detection results of the surveying line: (a) schematic diagram of electric field component interpretation, where (E) refers to “electric field component”; (b) schematic diagram of the comparison of electric field component for a single track; (c) photo of the leakage area at the surveying line.

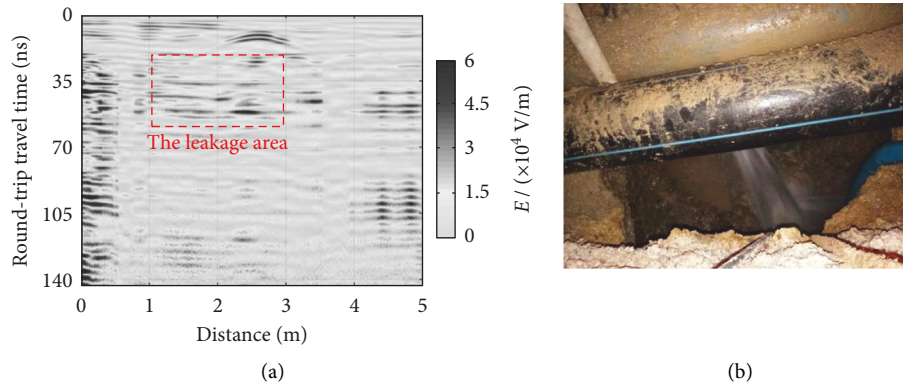


FIGURE 6: Detection results of the complementary line: (a) schematic diagram of electric field component interpretation, where (E) refers to “electric field component”; (b) photo of the leakage area at the complementary line.

The GPR profile of the surveying line is shown in Figure 4. It can be seen that a hyperbolic strong reflection area appears at the distance of 2.5–3.5 m and during the time period of 10–15 ns, which is inferred as a pipeline. In addition, there is a suspicious horizontal strong reflected wave below the pipeline, but this is affected by the horizontal signal at the time period of 40–60 ns. Meanwhile, at the distance of 9–18 m, the signal is relatively cluttered beginning from the time point of 40 ns, which leads to difficulties in the data interpretation.

The GPR data of the surveying line are interpreted using electric field component imaging, as shown in Figure 4.

The following can be seen from Figure 4: (1) A hyperbolic abnormal area appears at the upper left at the distance of 2.5–3.5 m and during the time period of 10–15 ns. In addition, the electric field component has a large amplitude, which is inferred to be an underground pipeline. (2) There is a horizontal high-amplitude area under the abovementioned hyperbolic anomaly, and the anomaly is likely caused by the water in the pipeline. (3) The event axis of the reflected wave at the distance of 1–3 m and during the time period of 25–70 ns is disordered (shown as the red box in Figure 5(a)). Furthermore, the amplitude of the electric field component is high and there is still an oscillating signal below the abnormal area. Considering that the place is located next to the pipeline, it is inferred that the abnormal area is the leakage area and the strong reflected wave is caused by underground water leakage. (4) There is a strong energy area within the distance of 14–18 m (shown as the blue box in Figure 6(a)), but the event axis of the reflected wave is continuous and regular. Therefore, it is inferred to be the subgrade structure.

The comparison diagram of the single-track electric field component curves of the 100-th track (distance of 2.5 m) and the 150-th track (distance of 3.75 m) is shown in Figure 6(b). It can be observed that the trends of the two electric field component curves are fundamentally similar, but the phase of the 100-th track is slightly delayed, and it is inferred that the water content at a distance of 2.5 m is higher.

For the verification of the abnormal area in Figure 5, a complementary line is arranged in parallel at the position 1 m on the left of the surveying line. Its electric field

component diagram of GPR data is shown in Figure 6. From Figure 6, it can be clearly identified that the pipes are located within a distance of 2–3 m. In addition, there is an abnormal area where the reflected wave has disordered events and strong energy at the distance of 1–3 m and at the time of 20–60 ns (shown as the red box in Figure 6(a)), which is inferred to be the leakage area. It can be seen that the detection results in Figure 6 are basically consistent with those in Figure 5.

5. Conclusion

Through theoretical analysis and experimental data verification, the following conclusions are drawn:

- (1) The relationship between the electric field component and the relative permittivity is derived in this paper. In addition, the forward simulation results of GPR are used to prove the theoretical basis that the greater the difference in permittivity is, the stronger the reflected wave energy will be.
- (2) According to the characteristics of high water content in the abnormal leakage area, electric field component imaging technology is used to analyze and explain the leakage detection of pipelines in an industrial area and the abnormal leakage area within the range of 1–3 m horizontal distance is delineated.
- (3) The electric field component imaging technology can clearly and accurately identify the abnormal leakage area, which exhibits the feasibility of this technology in leakage detection. However, the electric field component imaging technology is limited due the premise that there is a large dielectric difference between the target and the background medium. Therefore, the electric field component imaging technology can be used as an auxiliary means for conventional radar profile imaging.

Data Availability

The data that support the findings of this study are available from the corresponding author upon reasonable request.

Conflicts of Interest

The authors declare no conflicts of interest.

Acknowledgments

This research was supported by the National Natural Science Foundation of China (No. 42062015) and the Natural Science Foundation of Guangxi (No. 2018AD19204).

References

- [1] H. Dong, S. Liu, and C. Wang, "Study on near-surface water content measurement by ground-penetrating radar," *Journal of Jilin University (Earth Science Edition): Earth Science Edition*, vol. 39, no. 1, pp. 163–167, 2009.
- [2] L. Liu and R. Qian, "Ground-Penetrating Radar: a critical tool in near-surface geophysics," *Progress in Geophysics*, vol. 58, no. 8, pp. 2606–2617, 2015.
- [3] J. Xiong, M. Sun, and C. Peng, "The method for detection of town gas PE pipeline based on ground-penetrating radar," *Geophysical and Geochemical Exploration*, vol. 39, no. 5, pp. 1079–1084, 2015.
- [4] M. Yuan, "The capacity of the ground penetrating radar for detecting underground pipelines," *Geophysical and Geochemical Exploration*, vol. 26, no. 2, pp. 152–155, 2002.
- [5] C. Liu, J. Jiang, and Y. Yang, "Effect analysis of underground pipelines detection with the ground penetrating radar," *Journal of Shandong University of Science and Technology: Natural Science*, vol. 20, no. 1, pp. 57–60, 2001.
- [6] H. Xiao, W. Lei, and W. Yang, "Correspondence between geological characteristics of radar images and typical geological phenomenon," *Coal Geology & Exploration*, vol. 36, no. 4, pp. 57–61, 2008.
- [7] X. Wu, J. He, and J. Liu, "The effect of the electromagnetic wave's impedance transform to the results of the ground-probing-radar," *Progress in Geophysics*, vol. 21, no. 1, pp. 251–255, 2006.
- [8] B. He and X. Wei, "The forward modeling of drift pulled ahead exploration," *Coal Geology & Exploration*, vol. 28, no. 5, pp. 52–55, 2000.
- [9] D. Feng, Q. Dai, and J. He, "Finite difference time domain method of GPR forward simulation," *Progress in Geophysics*, vol. 21, no. 2, pp. 630–636, 2006.
- [10] Q. Dai, D. Feng, and Q. Wang, "The application of finite difference time domain method in the ground penetrating radar two-dimension forward simulation," *Progress in Geophysics*, vol. 19, no. 4, pp. 898–902, 2004.
- [11] Y. Zhu, Q. Wang, and Q. Zhang, "FDTD numeric technique-based analysis of the influence of reverse obstacle on data acquisition of ground penetrating radar," *Coal Geology & Exploration*, vol. 44, no. 5, pp. 149–154, 2016.